Proceedings of ISFOG 2025
5TH INTERNATIONAL SYMPOSIUM ON
FRONTIERS IN OFFSHORE GEOTECHNICS
Nantes, France | June 9-13 2025

ISBN 978-2-85782-758-0

Effect of shaft diameter on undrained bearing capacity of conical penetrometers/footings

Anish Pandit*
IITB-Monash Research Academy/Department of Civil Engineering/Indian Institute of Technology Bombay /Mumbai, India
Department of Civil & Environmental Engineering/Monash University/Clayton, Australia
Department of Civil Engineering/Indian Institute of Technology Bombay/Mumbai, India
Santiram Chatterjee
Department of Civil Engineering/Indian Institute of Technology Bombay/Mumbai, India
Ha Hong Bui
Department of Civil & Environmental Engineering/Monash University/Clayton, Australia
**anish.pandit@monash.edu*

ABSTRACT:
Many offshore foundation systems, such as spudcans, dynamically penetrating anchors, and various penetrometers, have a conical shape. When estimating the penetration resistance of these cones in clayey soil, understanding the undrained bearing capacity factors for cones with different apex angles is crucial. Existing literature primarily addresses the bearing capacity factors for conical footings placed in open trenches at varying embedment levels. However, in real-world applications, soil cover often exists above the foundation or penetrometer, a factor not accounted for in many earlier studies. Moreover, previous research often overlooked the impact of a thin shaft, commonly present above spudcans or penetrometers. This shaft, which can have a diameter equal to or smaller than the tip's diameter, plays a critical role in the penetration process. The presence of the shaft significantly alters the failure mechanism and the corresponding bearing capacity. This study numerically investigates the undrained bearing capacity factors for conical foundations or penetrometers, considering varying apex angles, shaft diameters, and embedment levels. The analysis also examines both frictionless and fully rough cone-soil interfaces. Results indicate that bearing capacity factor decreases with increasing shaft diameter and increases with roughness. Additionally, while bearing capacity factors rise sharply with the initial increase in embedment depth, they tend to stabilize as the depth increases. Comparison with previous research highlights the importance of considering soil cover and shaft diameter in the assessment of bearing capacity.

Keywords: Undrained, shaft diameter, bearing capacity, penetrometer, finite element analysis.

1.1 INTRODUCTION

Deepwater offshore sediments are typically fine-grained, and normally consolidated. These soils are generally very soft, and any load applied by offshore structures induces undrained conditions. Low hydraulic conductivity of deepwater sediments ensures undrained behaviour during rapid loading. Therefore, understanding the undrained bearing capacity of offshore foundations or different penetrometers on such sediments is of paramount importance. Foundations with conical shape or penetrometers with conical tip are very common in offshore applications for example spudcans, dynamically penetrating anchors. Previous studies on conical foundation systems focussed on various parameters influencing the undrained bearing capacity, such as the apex angle of the cone, depth of embedment, shear strength profile, and the roughness of the foundation or the penetrometer.

Houlsby & Martin (2003) explored the undrained bearing capacity of conical foundations placed inside a trench in clay, providing theoretical solutions for predicting bearing capacity factors. Their research offered fundamental insights into the behavior of conical foundations commonly used in offshore applications. Randolph & Gourvenec (2011) gave a comprehensive overview of offshore foundation systems, stressing the importance of understanding soil behavior under undrained conditions due to the soft, fine-grained sediments prevalent in deepwater offshore environment. Their work underscored the critical impact of soil shear strength profiles and embedment depth on bearing capacity. Nguyen & Chung (2015) studied the effect of area ratio of the ball penetrometer on the bearing resistance. The study shows that bearing resistance decreases with decreasing area ratio until it reaches a minimum value at a certain area ratio and then increases with further

decrease in area ratio. The results indicated that a larger area ratio gives higher undrained resistance because of the frictional resistance of the shaft. Zhou & Randolph (2015) conducted research to examine the effect of the shaft on the resistance of a ball penetrometer. Their study explored practical ball–shaft diameter ratios ranging from 2 to 5, including the extreme cases of a ball without a shaft and a shaft without a protruding ball. They found that the penetration resistance slightly decreases as the ball–shaft area ratio decreases, with a 4.4% reduction in resistance for an area ratio of 9 compared to the ideal case of no shaft. Their findings also revealed that the presence of the shaft results in only a minimal difference between extraction and penetration resistance.

Zhou et al. (2016) highlighted that the area ratio of the shaft to the ball penetrometer significantly influences the deep bearing factors and the critical penetration depth. Larger shaft diameters were found to overestimate the shear strength of the bottom layer in stiff-over-soft clay deposits. The study by Dutta & Haldar (2020) provides a comprehensive assessment of the uncertainty associated with undrained shear strength measurements of soft sediments using a ball penetrometer. By evaluating the variability in test results, the research highlights the critical factors influencing measurement accuracy and underscores the importance of considering these uncertainties in geotechnical analysis and design. The findings contribute to improved reliability in soft sediment characterization, offering valuable insights for engineering applications. Maleki et al. (2024) investigated the bearing capacity of deep foundations in liquefiable soils using data from piezocone penetration tests (CPTu). The authors focus on the impact of soil sensitivity and undrained shear strength on bearing capacity evaluations. This approach not only provides precise and continuous records but also enhances the reliability of geotechnical resistance estimates, making it a valuable tool in geotechnical engineering practices.

Previous literature has largely overlooked thin-shafted conical foundations or conical penetrometers when estimating undrained bearing capacity. A full flow free-fall penetrometer with conical tip (e.g. Chow & Airey (2014)) would typically have shaft thinner than its tip diameter. A full flow penetrometer with a plate-shaped tip would also have a thinner shaft. On the other hand, cone penetration test apparatus or a dynamically penetrating anchor would have equal diamters for shaft and tip. Considering these practical offshore applications, it is necessary to study the effect of varying shaft diameter on undrained bearing capacity of cones with different apex angles. Moreover, undrained bearing capacity factors for conical shapes were typically defined at various embedment depths in open trenches in the existing literature. However, in practical scenarios, soil cover is usually present over the foundations or penetrometers, which affects their bearing cpacity. This study aims to bridge this gap by examining the impact of shaft diameter—equal to or less than the cone tip diameter—on the undrained bearing capacity.

To better replicate practical conditions, this study analyzes closed trenches using wished-in-place conditions to calculate bearing capacity factors for conical shapes. The research also considers other critical factors, such as the cone tip angle (apex angle), depth of embedment, and interface properties between the soil and the foundation or penetrometer. By taking these parameters into account, the study seeks to provide a more comprehensive understanding of the undrained bearing capacity of conical offshore foundations and penetrometers.

2 NUMERICAL ANALYSIS

2.1 Geometry and Parameters

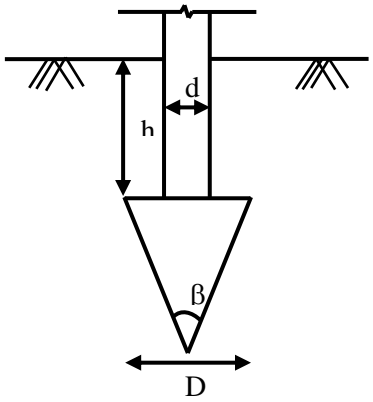

Figure 1. Problem Geometry

The study investigates a conical-shaped penetrometer/foundation designed to be wished in place. The diameter of the shaft above the tip varies relative to the diameter of the tip. To prevent any obstruction in the full flow mechanism, the shaft's diameter should be less than 15% of the tip diameter (Randolph & Gourvenec (2011), Nguyen & Chung (2015)). Therefore, a shaft diameter of 0.1D (where D is the cone tip diameter) is considered as the thin shaft and is varied up to 1D for the parametric analysis. The geometry of the penetrometer is illustrated in Figure 1. The soil is assumed to be homogeneous, isotropic with an undrained shear strength of 10 kPa. The current study focuses on a tip diameter (D) of 2 meters. The results are presented in terms of a non-dimensional bearing capacity factor, which remains consistent across other tested tip diameters. The normalized

depth of embedment (h/D) was varied from 0 to 2.5 to cover the range from global failure to the local failure mechanism. The apex angle (β) is also varied to evaluate its effect on the bearing capacity factors. The failure mechanism for different shaft diameters is also examined. Table 1 provides the parameters used for the analysis of the undrained bearing capacity of conical shapes.

Table 1. Values of parameters used for the study

Sr. No.	Parameter	Value
1	Cone Apex angle (β)	30˚, 60˚, 90˚, 180˚ (plate)
2	Depth of embedment (h/D)	0, 0.1, 0.25, 0.5, 1, 2.5
3	Shaft Diameter (d/D)	0.1, 0.25, 0.5, 0.75, 1.0
4	Interface	Frictionless/rough

2.2 Analysis Details

Small strain finite element analyses were conducted to determine the undrained bearing capacity factors using axisymmetric analyses within the Abaqus 6.14-2 software package. The Mohr-Coulomb soil constitutive model with zero friction angle was employed to define soil behavior, with specific details outlined in Table 2. To simulate undrained conditions in the soil, a Poisson's ratio of 0.495 (slightly less than 0.5 to prevent numerical errors) was selected. Young's modulus value equaling 500 times the undrained shear strength was assumed. The soil was assumed to be weightless, as the geotechnical bearing capacity factor remains unaffected by the soil unit weight (γ) for undrained capacities. The top portion of the cone was modelled as a no-separation interface to ensure continuous contact between the soil and the cone top during penetration.

A soil domain radius of 15D and height of 20D was chosen to mitigate boundary effects. The penetrometer was positioned within the soil domain at various embedment depths, treated as a rigid body by assigning a rigid body type constraint. Bearing capacity factors were determined for both frictionless and rough interfaces of the penetrometer. A prescribed displacement was applied to the penetrometer to reach the limiting resistance. Triangular mesh elements with a CAX6 configuration were utilized to discretize the model. For the soil domain, very fine mesh elements were employed near the penetrating object, while coarser meshing was used near the domain boundaries. Mesh convergence analysis indicated that a minimum mesh element size of 0.0025D (near the penetrating object) was optimal for obtaining results, while a mesh element size of 0.5D was chosen for elements near the boundaries. Figure 2 illustrates the meshing details for the model.

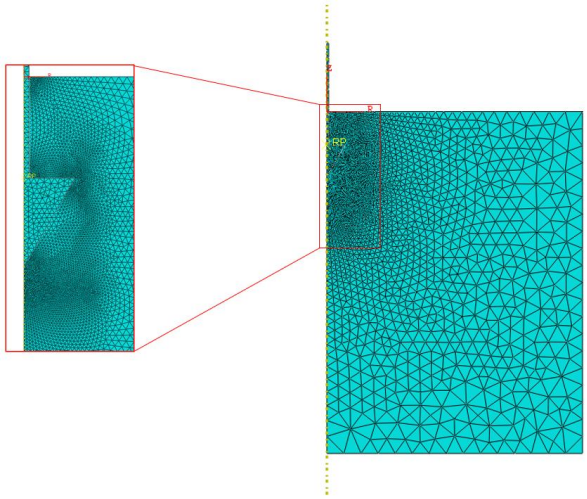

Figure 2. Typical mesh details for the penetrometer and soil

Table 2. Mohr-coulomb constitutive model details

Parameter	Value	Units
Undrained shear strength (s_u)	10	kPa
Young's modulus (E)	$500s_u$	kPa
Poisson's ratio (ν)	0.495	-
Friction angle (ϕ)	0	°
Dilation angle (ψ)	0	°

3 RESULTS AND DISCUSSION

3.1 Parametric Analysis

Detailed parametric study for a wide range of cone angles, shaft diameter and initial embedment ratios as mentioned in Table 1 was performed. At any particular embedment, the cone was pushed downward and the reaction from soil was recorded. After certain displacement, a steady state is reached where the vertical reaction force does not change with further displacement. The steady reaction (Q) is normalized with the projected area of the cone (A) and undrained shear strength of the soil to define bearing capacity factor as $N_{c0} = \mathrm{Q}/(\mathrm{A} \times s_u)$.

Figure 3 illustrates the impact of shaft diameter on undrained bearing capacity factors for h/D values of 0.5 and 1, across different apex angles for frictionless interface. Notably, for h/D = 0.5, the undrained bearing capacity factors do not decrease with some initial increases in shaft diameter, whereas for h/D = 1, the factors begin to decrease as soon as the shaft diameter starts increasing. Obtained results indicate that as the shaft diameter increases, the bearing capacity factor decreases. For instance, with h/D at 0.5 and an apex angle of 30˚, the undrained bearing

capacity factor decreases from 8.097 to 5.776 as the shaft diameter (d) increases from 0.1 D to 1 D. This demonstrates a 28.7% reduction in undrained bearing capacity due to the increase in shaft diameter. This reduction is attributed to a shift from a full-flow failure mechanism in thin shafts to a constrained-flow or cavity opening mechanism in full shafted penetrometers, as discussed later in the paper

It is noteworthy to mention that for full-shaft penetration, the plateau in the undrained bearing capacity against penetration depth was not reached even after a prescribed displacement of 50% of the penetrometer's diameter for deeply embedded penetrometers. Therefore, in such cases, an increased value of Young's modulus, equal to $1000s_u$, was adopted to achieve a plateau for the bearing capacity.

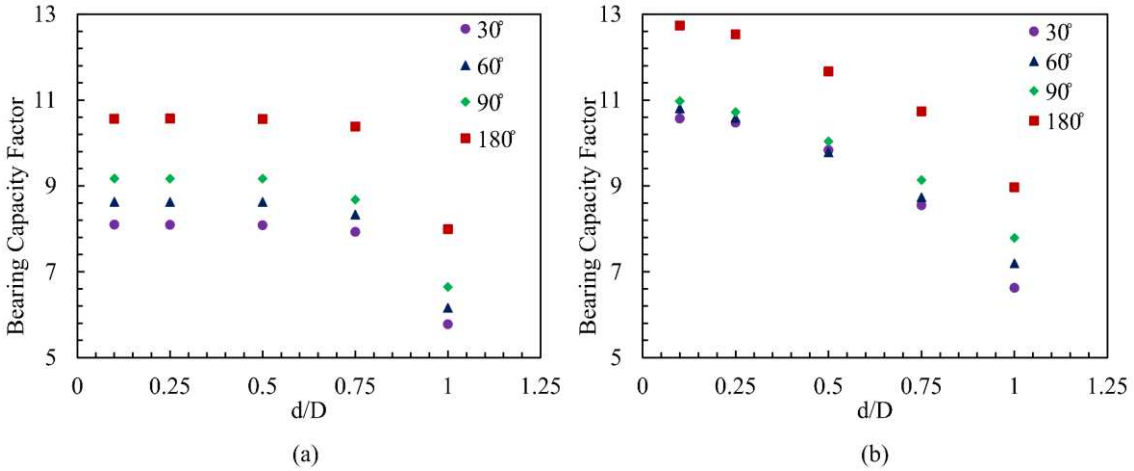

Figure 3. Undrained bearing capacity factor versus shaft diameter for (a) h/D = 0.5 & (b) h/D = 1

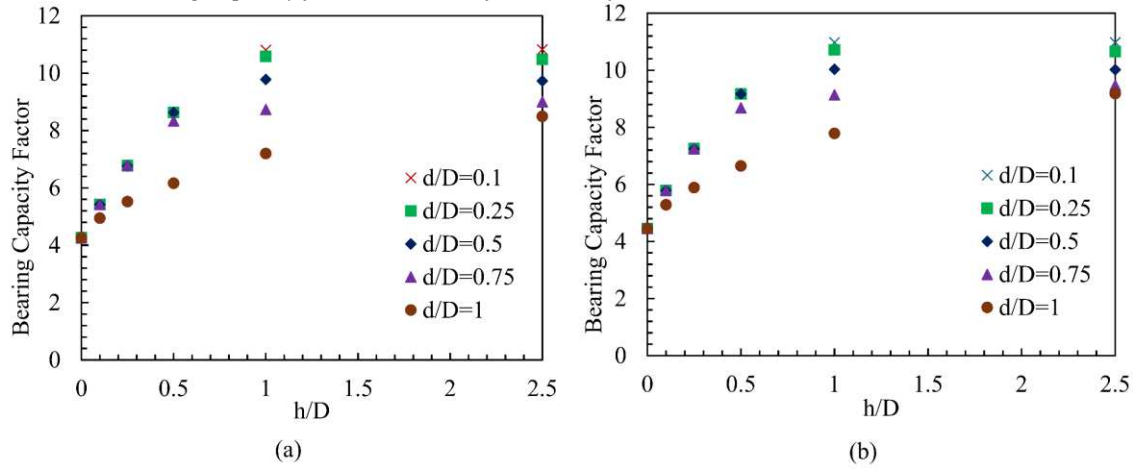

Figure 4. Undrained bearing capacity factor versus depth of embedment for different shaft diameter with (a) apex angle = 60° and (b) apex angle = 90°

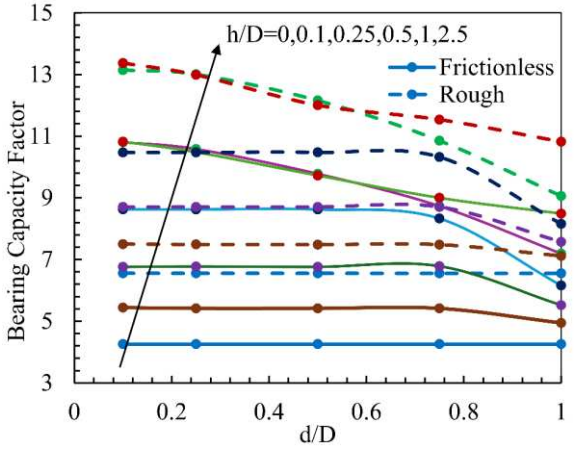

Figure 5. Comparison between the smooth and rough interfaces of the penetrometer with an apex angle of 60°

The curves for undrained bearing capacity factors against depth of embedment are plotted in Figure 4 to analyze the effect of embedment depth. These curves show that undrained bearing capacity factors increase with greater embedment depth, a well-documented trend. Notably, for thin-shafted penetrometers or foundations, the undrained capacity factors are similar for h/D = 1 and h/D = 2.5, indicating that a plateau has been reached and further increases in embedment depth would not raise the capacity factors. This suggests that for normalized shaft diameters (d/D) of 0.5 or less, penetration follows the same full-flow failure mechanism as thin-shafted penetrometers. However, for full-shafted penetrometers, the failure mechanism transitions to constrained flow, as evidenced by the continuous increase in undrained

capacity factor with greater embedment depth. For d/D = 0.75, there is a slight increase in the undrained capacity factor, indicating an intermediate failure mechanism or transition phase from full flow to constrained flow.

Interface roughness factor between the foundation surface and the soil depends on various facors, such as corrosion of the foundation material or the marine growth over the foundation. In the present study, fully smooth and fully rough interafce conditions are considered. Figure 5 shows that while the trend in bearing capacity factors remains largely unchanged, the bearing capacity itself increases with a rough interface, which is expected.

3.2 Failure Mechanism

As mentioned previously, the failure mechanism changes for thin-shafted to full-shafted penetrometers. This transition in failure mechanisms is also examined and highlighted in this section. For thin-shafted penetrometers, a full-flow type mechanism was observed, where the soil failing below the penetrometer accumulates on top of it. Figure 6 shows the displacement vectors for different shaft diameters, indicating a full-flow type failure mechanism for shafts up to a diameter of 50% of the tip diameter. The case with a shaft diameter of 25% is not shown here because the displacement vectors closely resemble those in the 10% shaft diameter case. In the 75% shaft diameter case, there appears to be some soil flowing back over the top of the penetrometer, but the mechanism is gradually transitioning from full-flow to a more constrained flow. This shift is clearly visible in the 100% shaft diameter case. For the penetrometer with a 100% shaft diameter, no soil flows back. As the penetrometer is pushed into the soil, it displaces the adjacent soil laterally, creating a cavity. Since this mechanism involves less soil displacement, it explains the lower bearing capacity factors observed in the full-shaft penetrometer case.

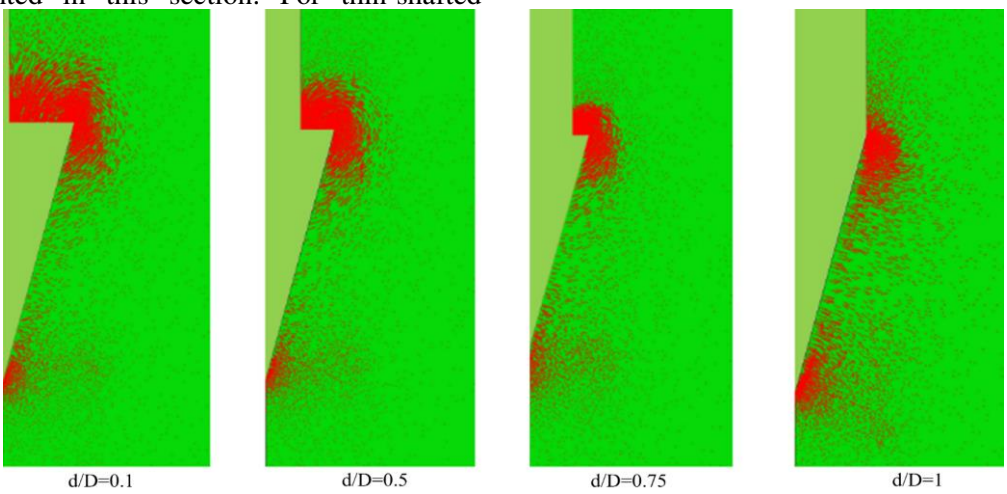

Figure 6. Displacement vectors for different shaft diameter

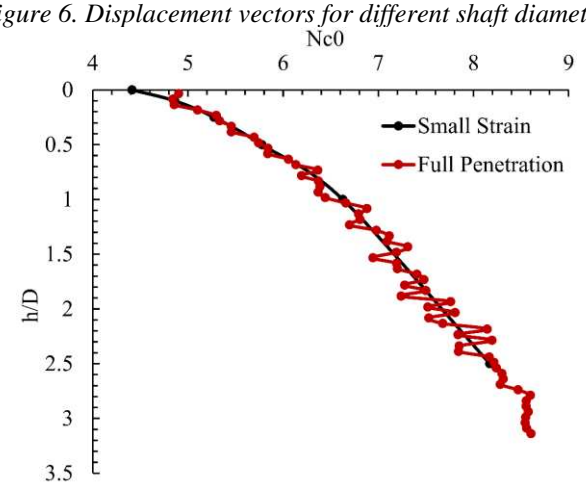

Figure 7. Evolution of bearing capacity factor with embedment depth for full shafted penetration

Additionally, full penetration analyses using the ALE (Arbitrary Lagrangian Eulerian) technique for full-shafted penetrometers were conducted alongside small strain analyses. The results of these analyses are plotted in Figure 7, showing a strong resemblance. Figure 7 indicates that for full-shafted penetration, the undrained bearing capacity factor does not stabilize but continuously increases as the penetrometer is pushed into the soil. This continuous increase is due to the cavity opening failure mechanism, which opens a cavity and pushes the soil away and upwards from the penetrometer, leading to an increase in the undrained bearing capacity factor.

Table 3 presents a comparison of the undrained bearing capacity factors from this study with those reported by Houlsby & Martin (2003) for the range of h/D considered and an apex angle of 60°. The bearing capacity factor lies fairly close to Houlsby & Martin (2003) for h/D=0 case. However, as h/D increases, the results begin to diverge due to the presence of soil cover above the penetrometer and the influence of shaft diameter, as discussed in this paper. The key differences in undrained bearing capacity factor from

both the studies indicate that the soil above the penetrometer tip enhances undrained resistance. However, a larger shaft diameter results in reduced bearing cpacity factor due to the change in failure mechanism.

Table 3. Comparison between the undrained bearing capacity factors from the present study and that from Houlsby and Martin (2003) for apex angle 60°

h/D	Houlsby & Martin (2003)	Present Study				
		Normalized Shaft diameter (d/D)				
		0.1	0.25	0.5	0.75	1
0	4.446	4.259	4.259	4.259	4.259	4.259
0.1	4.677	5.444	5.419	5.419	5.418	4.944
0.25	4.98	6.764	6.773	6.764	6.785	5.521
0.5	5.414	8.628	8.626	8.626	8.332	6.160
1	6.066	10.805	10.582	9.779	8.733	7.195
2.5	7.327	10.823	10.483	9.726	9.001	8.490

4 CONCLUSION

This study systematically explored the undrained bearing capacity factors of conical penetrometers with varying shaft diameters and embedment depths, uncovering critical insights into failure mechanisms. The findings indicate that the presence of soil cover increases the undrained bearing capacity and an increase in shaft diameter leads to a decrease in bearing capacity factors, with a notable 28.7% reduction observed when the diameter increases from 0.1 D to 1 D. This reduction is attributed to a shift from full-flow to constrained-flow or cavity opening mechanisms. Thin-shafted penetrometers exhibit a full-flow mechanism, where soil accumulates on top, while full-shafted penetrometers show a constrained-flow mechanism, characterized by outward and upward soil displacement forming a cavity. Additionally, rough interfaces increase bearing capacity without altering the overall trend. The presented bearing capacity factors would be useful for estimating undrained shear strength using conical penetrometers or bearing capacity of conical foundations.These insights are crucial for designing penetrometers and foundations, emphasizing the need to consider shaft diameter and embedment depth to accurately predict bearing capacity and understand failure mechanisms.

AUTHOR CONTRIBUTION STATEMENT

A. Pandit: Data curation, Formal Analysis, Writing- Original draft. **S. Chatterjee**.: Methodology, Visualization, Supervision, Writing- Reviewing and Editing. **H. H. Bui**: Supervision, Writing- Reviewing and Editing.

REFERENCES

Chow, S. H., & Airey, D. W. (2014). Free-Falling Penetrometers: A laboratory investigation in clay. *Journal of Geotechnical & Geoenvironmental Engineering, 140*(1), 201-214.

Dutta, D., & Haldar, S. (2020). Assessment of Uncertainty of Undrained Shear Strength of Soft Clay Using Ball Penetrometer. Í S. Haldar, S. Patra, & R. Ghanekar (Ritstj.), *Advances in Offshore Geotechnics. Lecture Notes in Civil Engineering. 92.* Singapore: Springer. doi:10.1007/978-981-15-6832-9_24

Houlsby, G. T., & Martin, C. (2003). Undrained bearing capacity factors for conical footings on clay. *Geotechnique, 53*(5), 513-520. doi:10.1680/geot.53.5.513.37507

Maleki, M., Eslami, A., Nabizadeh, A., & Bahmanpour, A. (2024). Bearing Capacity Evaluation of Deep Foundations in Liquefiable Soils Using Piezocone Test Data. *Geotechnical and Geological Engineering*. doi:10.1007/s10706-024-02885-3

Nguyen, T. D., & Chung, S. G. (2015). Effect of shaft area on ball resistances in soft clays. *Proceedings of the Institution of Civil Engineers-Geotechnical Engineering. 168*, bls. 103-119. ICE. doi:10.1680/geng.14.00023

Randolph, M., & Gourvenec, S. (2011). *Offshore Geotechnical Engineering.* CRC Press.

Randolph, M., Stanier, S., O'Loughlin, C., Chow, S., Bienen, B., Doherty, J., . . . White, D. (2018). *Penetrometer equipment and testing techniques for offshore design of foundations, anchors and pipelines.* CRC Press.

Zhou, H., & Randolph, M. (2015). Effect of shaft on resistance of a ball penetrometer. *Geotechnique, 61*(11), 973-981. doi:10.1680/geot.9.P.062

Zhou, M., Hossain, M. S., Hu, Y., & Liu, H. (2016). Scale Issues and Interpretation of Ball Penetrationin Stratified Deposits in Centrifuge Testing. *Journal of Geotechnical and Geoenvironmental Engineering, 142*(5). doi:10.1061/%28ASCE%29GT.1943-5606.0001442